Differentiation of Bacterial and Non-bacterial Community-acquired Pneumonia by Thin-section Computed Tomography

Isao Ito, MD, PhD
Tadashi Ishida, MD, PhD, FCCP
Kaori Togashi, MD, PhD
Akio Niimi, MD, PhD
Hiroshi Koyama, MD, PhD
Takayoshi Ishimori, MD, PhD
Hisataka Kobayashi, MD, PhD
Michiaki Mishima, MD, PhD

From the Departments of Respiratory Medicine (Drs. Ito and Ishida), and Radiology (Dr. Ishimori), Kurashiki Central Hospital, Kurashiki, Japan; the Departments of Respiratory Medicine (Drs. Ito, Niimi and Mishima), Clinical Epidemiology (Dr. Koyama), and Diagnostic Imaging and Nuclear Medicine (Drs. Togashi and Kobayashi), Kyoto University, Kyoto, Japan; and Molecular Imaging Program, Center for Cancer Research, National Cancer Institute, National Institutes of Health, MD, USA (Dr. Kobayashi).

Corresponding author:
Isao Ito, MD, PhD
Department of Respiratory Medicine, Kyoto University,
54 Shogoin-kawaharacho, Sakyo-ku, Kyoto, 606-8507, Japan
Phone: 81-75-751-3884, Fax: 81-75-751-4643,
E-mail: isaoito@kuhp.kyoto-u.ac.jp

Addresses of co-authors

Tadashi Ishida, MD, PhD, FCCP
Department of Respiratory Medicine, Kurashiki Central Hospital,
1-1-1　Miwa, Kurashiki, 710-8602, Japan.
Phone: 81-86-422-0210, Fax: 81-86-421-3424,
E-mail: ishidat@kchnet.or.jp

Kaori Togashi, MD, PhD
Department of Diagnostic Imaging and Nuclear Medicine, Kyoto University,
54 Shogoin-kawaharacho, Sakyo-ku, Kyoto, 606-8507, Japan.
Phone: 81-75-751-3760, Fax: 81-75-751-9709,
E-mail: ktogashi@kuhp.kyoto-u.ac.jp

Akio Niimi, MD, PhD
Department of Respiratory Medicine, Kyoto University,
54 Shogoin-kawaharacho, Sakyo-ku, Kyoto, 606-8507, Japan.
Phone: 81-75-751-3884, Fax: 81-75-751-4643,
E-mail: niimi@kuhp.kyoto-u.ac.jp

Hiroshi Koyama, MD, PhD
Department of Clinical Epidemiology, Kyoto University,
54 Shogoin-kawaharacho, Sakyo-ku, Kyoto, 606-8507, Japan.
Phone: 81-75-751-4246, Fax: 81-75-751-4223,
E-mail: hkoyama@kuhp.kyoto-u.ac.jp

Takayoshi Ishimori, MD, PhD
Department of Radiology, Kurashiki Central Hospital,
1-1-1　Miwa, Kurashiki, 710-8602, Japan.
Phone: 81-86-422-0210, Fax: 81-86-421-3424
E-mail: ti10794@kchnet.or.jp

Hisataka Kobayashi, MD, PhD
Molecular Imaging Program, Center for Cancer Research, National Cancer Institute,
National Institutes of Health
Bldg. 10, Room 1B40, MSC1088, 10 Center Dr., Bethesda, MD 20892-1088, USA

Phone: 1-301-435-4086, Fax: 1-301-402-3191
E-mail: kobayash@mail.nih.gov

Michiaki Mishima, MD, PhD
Department of Respiratory Medicine, Kyoto University,
54 Shogoin-kawaharacho, Sakyo-ku, Kyoto, 606-8507, Japan
Phone: 81-75-751-3884, Fax: 81-75-751-4643
E-mail: mishima@kuhp.kyoto-u.ac.jp

Differentiation of Bacterial and Non-bacterial Community-acquired Pneumonia by Thin-section Computed Tomography

ABSTRACT

***Background and objective*:** The management of community-acquired pneumonia (CAP) depends, in part, on the identification of the causative agents. The objective of this study was to determine the potential of thin-section computed tomography (CT) in differentiating bacterial and non-bacterial pneumonia.

***Patients and methods*:** Thin-section CT studies were prospectively examined in hospitalized CAP patients within two days of admission, followed by retrospective assessment by two pulmonary radiologists. Thin-section CT findings on the pneumonias caused by each pathogen were examined, and two types of pneumonias were compared. Using multivariate logistic regression analyses, receiver operating characteristic (ROC) curves were produced.

***Results*:** Among 183 CAP episodes (181 patients, 125 men and 56 women, mean age ±SD: 61.1 ± 19.7) examined by thin-section CT, the etiologies of 125 were confirmed (94 bacterial pneumonia and 31 non-bacterial pneumonia). Centrilobular nodules were specific for non-bacterial pneumonia and airspace nodules were specific for bacterial pneumonia (specificities of 89% and 94%, respectively) when located in the outer lung areas. When centrilobular nodules were the principal finding, they were specific but lacked sensitivity

for non-bacterial pneumonia (specificity 98% and sensitivity 23%). To distinguish the two types of pneumonias, centrilobular nodules, airspace nodules and lobular shadows were found to be important by multivariate analyses. ROC curve analysis discriminated bacterial pneumonia from non-bacterial pneumonia among patients without underlying lung diseases, yielding an optimal point with sensitivity and specificity of 86% and 79%, but was less effective when all patients were analyzed together (70% and 84%).

***Conclusion*:** Thin-section CT examination was applied for the differentiation of bacterial and non-bacterial pneumonias. Though showing some potential, this examination at the present time would not be applicable for patients with underlying lung diseases, severe conditions of pneumonia, or immunocompromised conditions.

Key words:
Non-bacterial Pneumonia,
Bacterial Pneumonia,
High-resolution Computed Tomography,
Mycoplasmal Pneumonia,
Pneumococcal Pneumonia,

INTRODUCTION

Community-acquired pneumonia (CAP) is one of the most common acute lung diseases detected by radiographic abnormalities. In the management of CAP, pneumonias have been categorized into two groups based on sensitivity to antibiotics: bacterial pneumonia, which responds to the beta-lactam antibiotics, and non-bacterial pneumonia, which is non-responsive. Although new macrolides and new quinolones are considered to be effective therapeutic agents for non-bacterial pneumonias as well as for most of bacterial pneumonias, the recent emergence and spread of bacteria resistant to these drugs, especially in Asia including Japan, have raised significant worldwide concern [1, 2]. Therefore, the differentiation of these two types of pneumonias is recommended in the guidelines for the management of CAP from the Japanese Respiratory Society [3]. However, even the combined study of clinical manifestations and laboratory screenings such as blood cell counts and serum chemistries have yielded no information specific to either type of pneumonia. Moreover, studies on chest radiography have also failed to elucidate any precise differences [4].

Recent advances in computed tomography (CT) are now enabling the evaluation of normal or questionable radiographic findings [5]. Thin-section CT improves the

characterization of parenchymal infections and their complications in the management of lung infections [6]. In recent years, investigators have focused on radiologic findings of pneumonia caused by specific pathogens such as *mycoplasma* and *chlamydia* and the characteristics of these pneumonias have been described [5, 7-9]. During the recent epidemic of severe acute respiratory syndrome (SARS), the use of chest CT in combination with clinical findings was reported to be useful in ruling out a number of differential diagnoses [10]. Thin-section CT may have advantages over conventional chest radiography in the etiologic diagnosis of CAP. However, we are not aware of any prospective study investigating the usefulness of thin-section CT as a possible modality for distinguishing the different pathogens of pneumonia. The aim of this study was to elucidate the differences in thin-section CT findings between bacterial and non-bacterial pneumonia. As a part of this study, differences between two representative forms of CAP, i.e., pneumococcal pneumonia and mycoplasmal pneumonia, were also examined [11].

METHODS

Patients

Patients enrolled in the present thin-section CT study were part of our ongoing long-term, prospective study to detect etiological microorganisms in CAP cases at our hospital (a general teaching hospital with 1,151 beds) since July 1994 [11]. The present study was conducted between January 1998 and June 2001. The candidates for enrollment were the same candidates from the etiological study reported previously, i.e., all hospitalized CAP patients over 15 years of age [11]. CAP patients were designated as those who developed symptoms outside of any hospital or healthcare institution and presented with symptoms of respiratory infection such as cough, sputum or dyspnea, and infiltrate on chest radiography. Conventional chest CT and thin-section CT evaluations were performed on the hospitalized CAP patients who gave their informed consent. Prior to the study, the protocol was approved by the institutional review board. Patients were excluded from this study if they had at least one of the following conditions: inability to hold one's breathing sufficiently to perform a chest CT, shock, consciousness disturbance, thoracic deformity, an underlying lung disease (pulmonary emphysema, bronchiectasis, interstitial pneumonia, old tuberculosis, etc.) that could skew the thin-section CT findings, an underlying

immunodeficiency and possible pregnancy. Patients with lung diseases that were localized apart from pneumonia or minor underlying lung diseases that were not considered to affect the thin-section CT findings were included.

A total of 390 patients (273 men and 117 women) who had experienced 403 episodes of CAP were enrolled in this study. Among the 403 CAP cases, 288 (285 patients) were examined by chest CT. Next, 183 cases (181 patients, 125 men and 56 women, mean age ±SD: 61.1 ± 19.7) that did not qualify for the exclusion criteria described below in the section on *Chest thin-section CT study* were examined by thin-section CT, and the thin-section CT findings were assessed by two radiologists.

Determination of the causative microorganisms

Microbiological and serological studies were performed on all hospitalized CAP patients as described previously [11]. Pneumonias caused by *Streptococcus pneumoniae* (*S. pneumoniae*) or other bacteria were diagnosed based on at least one of the following tests: blood culture, culture of needle aspiration fluid from pleural effusion or lung, quantitative culture of sputum or bronchoalveolar lavage fluid, and urinary antigen test (Binax NOW® *S. pneumoniae* Urinary Antigen Test, Binax, Portland, ME). Specific serological methods

were employed for diagnosis of non-bacterial pneumonias [12]. Pneumonia caused by *Mycoplasma pneumoniae* (*M. pneumoniae*) was diagnosed by a four-fold rise in the antibody titers (passive hemagglutinin test or complement fixation test) or by culture of sputum or pharyngeal swab [13].

Among the 183 cases examined by thin-section CT, 65 (63 patients) were diagnosed as pneumococcal pneumonia (including 6 co-infected with other organisms), 20 (20 patients) were diagnosed as mycoplasmal pneumonia, 43 were diagnosed as other infections, and 55 could not be etiologically confirmed (Table 1). Causal microorganisms were categorized into two types of pathogens: bacterial (*Streptococcus* spp., *Haemophilus influenzae* [*H. influenzae*], *Moraxella catarrhalis*, *Escherichia coli*, *Staphylococcus aureus*, anaerobes and *Klebsiella pneumoniae*) and non-bacterial (*M. pneumoniae*, *Chlamydia* spp., *Influenza* virus and *Measles* virus) [4, 6]. Before the analysis, clinicians excluded 3 cases: one who turned out to be co-infected with both bacterial and non-bacterial pathogens, one diagnosed with *Legionella* pneumonia and one with tuberculosis. Thus, the final analysis included etiologically confirmed thin-section CT findings on 94 bacterial and 31 non-bacterial pneumonias, including 59 pneumococcal and 20 mycoplasmal pneumonias. Radiologists diagnosed minor underlying lung diseases in 42 of the 183 CAP cases

examined by thin-section CT (25 with emphysema, 9 with lung fibrosis, 4 with old tuberculosis, 3 with bronchiectasis, and 1 with lung cancer).

Chest thin-section CT study

Conventional chest CT and thin-section CT scans were performed within 2 days of hospital admission (mean 1.1 days) with the patient in a supine position. One of the following three scanners was used: HiSpeed Advantage (General Electric Medical Systems, Milwaukee, WI), PQ5000 (Picker International, Cleveland, OH), or Asteion (Toshiba Medical Systems, Tokyo, Japan). All images were routinely obtained with 8- to 10-mm collimation at 10-mm intervals. Patients who were unable to hold their breath or found to have an underlying lung disease causing marked distortion of the lung architecture, massive pleural effusion causing passive atelectasis, or empyema on the routine chest CT examination were excluded from further thin-section CT study. The thin-section CT images were obtained with 1- to 3-mm collimation at 10 mm intervals, at a field of view of 20 cm. The images were reconstructed using a high-spatial-frequency algorithm and photographed at window settings for evaluation of the lung parenchyma (–700 HU [level] and 1,500 to 1,800 HU [width]) and the mediastinum (10 HU [level] and 300 HU [width]). Intravenous

contrast medium was not used.

Image analysis

Image analysis was done retrospectively following prospective enrollment of the patients and collection of the CT images. Hard copies of chest CT scan images were read on film and were assessed separately by two experienced chest radiologists blinded to the patients' data, clinical conditions, and chest roentogenography. After their independent readings, any differences in findings were checked. They then re-assessed the films in question together and final decisions were reached by consensus. The radiologists assessed the presence, location, and extent of the findings according to the previously reported descriptions [6, 14]. Areas of air-space consolidation (AS), areas of ground-glass attenuation (GG), lobular opacity, airspace nodules, centrilobular nodules, and thickening of bronchovascular bundles were assessed at the window setting for the lung parenchyma. Lobar pneumonia was defined as AS, GG or a mixture of the two occupying more than 70% of the area of one lobe. Mediastinal adenopathy (larger than 10 mm) and pleural effusion were assessed at the window setting for the mediastinum. The criteria for interpreting the findings are summarized in Table 2.

To assess the location of each radiological finding for thin-section CT, the lung parenchyma from the mediastinum to the pleura was divided into three zones of equal width (inner, middle and outer zones). Thin-section CT findings of areas of AS, GG, lobular opacity, airspace nodules, and centrilobular nodules were each classified into three distributional patterns, based on the predominant locations of each type of shadow. Each type of shadow was also assessed to determine whether it appeared unilaterally or bilaterally.

Statistical analysis

To identify the candidate radiological predictors for bacterial pneumonia versus non-bacterial pneumonia, and for pneumococcal pneumonia versus mycoplasmal pneumonia, statistical differences in the frequencies and distributions of thin-section CT findings were determined by either the chi-square test or Fisher's exact probability test. A $p < 0.05$ was considered to indicate statistical significance. Candidate predictors with $p < 0.10$ were selected and used in multivariate logistic regression analysis to construct the prediction equations for bacterial pneumonia versus non-bacterial pneumonia (model 1, with or without underlying lung diseases; model 2, without underlying lung diseases), and

pneumococcal pneumonia versus mycoplasmal pneumonia (model 3). Standard errors (SE), p-values of the likelihood ratio test, and estimated coefficients for independent variables (β) were determined. Probabilities of bacterial pneumonia (model 1 and 2) and pneumococcal pneumonia (model 3) were calculated for all patients in each group using the logistic model $P = 1 - 1/(1 + e^{r})$ and $r = [k + \Sigma\beta_i \times (0 \text{ or } 1)]$. The receiver operating characteristic (ROC) curves were generated using the models. StatView® version 5.0 (SAS Institute Inc., Cary, NC) was used for all of the statistical calculations. The degree of interobserver agreement between the two readers was assessed with the κ statistic: poor, κ= 0-0.20; fair, κ= 0.21-0.40; moderate, κ= 0.41-0.60; good, κ= 0.61-0.80; excellent, κ= 0.81-1.00.

RESULTS

Thin-section CT findings

Table 3 shows the frequency of thin-section CT findings in each etiological group. No specific findings predictive of certain organisms were found. The only difference between thin-section CT manifestations of *H. influenzae* pneumonia and pneumococcal pneumonia was in the detection of lobar pneumonia: zero out of 12 (0%) in the former vs. 20 out of 59 (34%) in the latter. Thin-section CT findings on chlamydial pneumonia were non-specific, with relatively less frequent airspace nodules, lobular opacity, and centrilobular nodules compared to mycoplasmal pneumonia. However, in comparing bacterial and non-bacterial pneumonia, several of the findings were found to occur at significantly different frequencies. Lobular opacity, centrilobular nodules, and thickening of bronchovascular bundles (BVB) were more frequent in non-bacterial pneumonia (p=0.002, p=0.001 and p=0.001, respectively) (Fig. 1-3). Prominent centrilobular nodules appeared as the main shadow more frequently in non-bacterial pneumonia cases in 7 out of 31 (23%) (p=0.001), with a specificity of 98% (92 out of 94) (Fig. 2). Areas of AS and areas of 'GG located around AS' were more frequently observed in bacterial pneumonia (p=0.017 and p=0.039) (Fig. 4), but these findings were non-specific. Airspace nodules in bacterial

pneumonia (Fig. 5) and centrilobular nodules in non-bacterial pneumonia (Fig. 3) tended to be located in the outer areas of the lung parenchyma (p=0.023 and p=0.001), with high specificities of 94% (29 out of 31) and 89% (84 out of 94) despite low sensitivities of 26% (24 out of 94) and 39% (12 out of 31), respectively. Bilateral centrilobular nodules were seen more frequently in non-bacterial pneumonia (p=0.007), with a sensitivity of 32% (10 out of 31) and specificity of 90% (85 out of 94). Interlobular septal thickening tended to be seen more often in bacterial pneumonias (p=0.087) (Fig. 6). The interobserver agreements (κ statistics) for the thin-section CT findings were 0.68 for centrilobular nodules, 0.50 for airspace nodules, 0.53 for lobular opacity, 0.71 for areas of AS, and 0.64 for areas of GG.

Multivariate logistic analysis

Table 4 shows three logistic regression models of the dependent variables using independent thin-section CT predictor findings: “bacterial pneumonia” in models 1 and 2, and "pneumococcal pneumonia" in model 3. Six independent variables were used to compose the models of probabilities for the presence of the dependent variables. The R^2 of the models 1, 2 and 3 were 0.299, 0.395 and 0.609. Figure 7 shows the ROC curves of the models described in Table 4. The areas under the ROC curves for the three models in Table

4 were 0.837, 0.885 and 0.953. The optimal points on the ROC curves to discriminate between bacterial and non-bacterial pneumonias in models 1 and 2 were obtained at P of 0.15 and 0.35, with sensitivities of 70% and 86%, and false positive ratios of 16% and 21%, respectively. The optimal point to discriminate between pneumococcal pneumonia and mycoplasmal pneumonia in model 3 was obtained at a P of 0.65, with a sensitivity of 94% and a false positive ratio of 15%.

DISCUSSION

We have demonstrated that thin-section CT can differentiate the two types of CAPs with reasonable accuracy in selected cases without underlying lung diseases. However, large numbers of patients had to be excluded from our analysis to obtain the optimal distinction of the two types. Previous investigations showed that bacterial and non-bacterial pneumonias could not be reliably distinguished by clinical presentation and chest radiography [4]. While there has been increased awareness of the utility of thin-section CT in the diagnosis of many lung diseases, including infectious cases, the role of thin-section CT in the etiological diagnosis of CAP remains to be established**.**

To our knowledge, only a few studies have evaluated the ability of thin-section CT to confirm the differentiation of pneumonia cases with established etiologies [5, 6, 8, 9]. Tanaka *et al.* showed that the frequencies of several thin-section CT findings differed significantly between two types of pneumonia. Moreover, the thin-section CT findings generally correlated well with pathogenesis and pathological findings [6]. In a study that covered both immunocompetent and immunocompromised patients, Reittner *et al.* concluded that thin-section CT is of limited value in the differential diagnosis of infective pneumonias, even though the pneumonias caused by *M. pneumoniae* and *Pneumocystis*

carinii exhibited characteristic appearances in thin-section CT [5]. In previous studies, because the decisions to perform CT scans were made mostly by clinical judgment and thin-section CT studies in CAP were not performed prospectively [5, 6, 8, 9], the problem of selection bias needs to be considered. Two types of selection bias are involved**:** bias in selecting the examination with which to detect the causative organisms, and bias in selecting the cases to undergo thin-section CT on the basis of already known clinical information and roentgenological findings. The present study was conducted in a prospective manner in order to minimize these biases. Moreover, this study has fulfilled a need in providing a description of thin-section CT findings on pneumonias caused by the common pathogens *S. pneumoniae* and *H. influenzae* which had not been adequately described in previous thin-section CT reports.

Classical studies using experimental models [15] and pathological findings [16] can be helpful in explaining the thin-section CT findings of pneumococcal pneumonia in our study, which detected an inflammatory response with an outpouring of edematous fluid that rapidly spread into the adjacent parenchyma. ‘Areas of GG around AS’, a finding described in pneumococcal pneumonia by Reittner [5], was more commonly found in bacterial pneumonia than in non-bacterial pneumonia in our study. This may be due to the

progression of the inflammation in bacterial pneumonias. On the other hand, the primary pathologic lesions of mycoplasma infection are known to be limited to the ciliated respiratory epithelium from the trachea to the bronchioles [15]. This propensity of mycoplasma infection to affect the airways has been shown in histopathological [17] and radiological [5, 7, 18, 19] studies. Our data on centrilobular nodules corroborated a study by Reittner, who observed the nodules in 96% of *M. pneumoniae* pneumonias and in 100% of viral pneumonias, versus only 17% of bacterial pneumonias [5]. Conceivably, centrilobular nodules are specific to non-bacterial pneumonias when seen as the prominent finding (specificity of 98%), bilaterally (90%), or predominantly in the outer lung zone (89%), inasmuch as none of these localizations showed high sensitivity (23%, 39% and 32%, respectively). Patients with *H. influenzae* pneumonia often have chronic obstructive pulmonary disease, and the saprophytic bacteria within the bronchial epithelium of these cases may trigger episodes of bronchopneumonia [16]. A pathologic pattern of air-space pneumonia similar to that in pneumococcal pneumonia can also occur [16]. The only detectable difference between pneumococcal pneumonia and *H. influenzae* pneumonia in our study was the appearance of lobar pneumonia (0% versus 34% frequency, respectively). Chlamydial pneumonia showed similarities and differences with mycoplasmal pneumonia

in thin-section CT findings [8, 9]. The disease showed a wide range of non-specific thin-section CT findings including both airspace pneumonia and bronchopneumonia. A histological investigation in an experimental model of Chlamydial pneumonia revealed inflammatory cell infiltration within the interstitium and alveolar space, accompanied by perivascular and peribronchiolar lymphoid cell accumulations [20].

We recognize that the possibility of selection bias was not entirely eliminated, since thin-section CT was not performed on the following: patients with mild pneumonias treatable at our outpatient clinic, patients with normal chest roentogenograms in spite of respiratory symptoms, and a substantial number of cases were excluded after conventional CT scan. Further, thin-section CT examination was inapplicable to various subgroups of patients, including those with severe conditions that prevented them from holding their breath, those suffering from underlying diseases with marked distortion of the lung architecture, and those with immunocompromised conditions. Chronic obstructive pulmonary disease was one of the most frequent co-morbidities in hospitalized patients with CAP (16%) [11]. Many of these were not included in this study in order to avoid misinterpretation of thin-section CT findings. In patients with immunodeficiency, a wider range of microorganisms including *Pneumocystis jirovecii*, *Aspergillus* and *Mycobacteria*

can cause pneumonia [5]. Consequently, six immunocompromised patients were excluded from the CT study. Investigation of immunocompromised patients is obviously needed to determine whether thin-section CT would be useful in differentiating causative organisms and should be analyzed separately from immunocompetent patients. Moreover, we were not able to evaluate CT findings of *Legionella* pneumonia because we had estimated at the outset of this study that we would have only a small number of *Legionella* cases that are more frequently encountered in Western countries based on previously reported studies [11,21]. Regarding methodology, using modern picture achieving and communication systems with narrower image intervals could have enabled more accurate evaluations of the images compared to using hard-copy films. Finally, the multivariate logistic regression model employed in this study was laborious and not entirely appropriate in the daily clinical setting. Further studies in which thin-section CT findings of pneumonia are evaluated by a simpler method are clearly needed.

For thin-section CT examination to be adopted for CAP patients, the additional radiation dose and increased operational costs will need to be considered. While CT evaluation is expected to help us in narrowing the differential diagnosis in selected CAP patients, we cannot suggest the routine clinical use of this modality until its impact on

clinical outcome and cost effectiveness are carefully evaluated.

In conclusion, our results indicate that variables obtained by thin-section CT findings could help in differentiating bacterial and non-bacterial pneumonias in appropriately selected cases with the application of logistic models. However, applying thin-section CT would be difficult in patients with underlying lung diseases, severe pneumonia or under immunocompromised conditions, which limit the usefulness of the examination. Although nothing specific was found for predicting a certain pathogen, the presence of air space nodules or centrilobular nodules and data on their localization and distribution were specific predictors for both types of pneumonia.

ACKNOWLEDGEMENT

We appreciate the efforts of Drs. Toru Hashimoto, Machiko Arita, Makoto Osawa and Hiromasa Tachibana in the Department of Respiratory Medicine, Kurashiki Central Hospital (KCH) for their recruiting and care of patients and for their suggestive discussions with us. We also thank Mr. Toshiharu Hongo in the Department of Laboratory Medicine in KCH for his help in laboratory tests, Dr. Yuji Watanabe, Director in the Department of Radiology in KCH for his role in the setting of CT examinations, Drs. Takeshi Kubo and Asako Nakai in the Department of Diagnostic Imaging and Nuclear Medicine in Kyoto University for their radiological assessments/discussions, and Mr. Simon Johnson for his linguistic help in writing the manuscript.

REFERENCES

1. Peterson LR. Penicillins for treatment of pneumococcal pneumonia: does in vitro resistance really matter? Clin Infect Dis 2006;42:224-33.

2. Inoue M, Kaneko K, Akizawa K, et al. Antimicrobial susceptibility of respiratory tract pathogens in Japan during PROTEKT years 1-3 (1999-2002). J Infect Chemother 2006;12:9-21.

3. Yanagihara K, Kohno S, Matsusima T. Japanese guidelines for the management of community-acquired pneumonia. Int J Antimicrob Agents 2001;18 Suppl 1:S45-8.

4. Tew J, Calenoff L, Berlin BS. Bacterial or nonbacterial pneumonia: accuracy of radiographic diagnosis. Radiology 1977;124:607-612.

5. Reittner P, Ward S, Heyneman L, Johkoh T, Muller NL. Pneumonia: high-resolution CT findings in 114 patients. Eur Radiol 2003;13:515-521.

6. Tanaka N, Matsumoto T, Kuramitsu T, et al. High resolution CT findings in community-acquired pneumonia. J Comput Assist Tomogr 1996; 20:600-608.

7. Reittner P, Müller NL, Heyneman L, et al. *Mycoplasma pneumoniae* pneumonia: radiographic and high-resolution CT features in 28 patients. Am J Roentogenol 2000;174:37-41.

8. Nambu A, Saito A, Araki T, et al. Chlamydia pneumoniae: comparison with findings of Mycoplasma pneumoniae and Streptococcus pneumoniae at thin-section CT. Radiology 2006;238:330-8.

9. Okada F, Ando Y, Wakisaka M, Matsumoto S, Mori H. Chlamydia pneumoniae pneumonia and Mycoplasma pneumoniae pneumonia: comparison of clinical findings and CT findings. J Comput Assist Tomogr 2005;29:626-32.

10. Müller NL, Ooi GC, Khong PL, Nicolaou S. Severe acute respiratory syndrome: radiographic and CT findings. Am J Roentogenol 2003;181:3-8.

11. Ishida T, Hashimoto T, Arita M, Ito I, Osawa M. Etiology of community-acquired pneumonia in hospitalized patients: a 3-year prospective study in Japan. Chest 1998;114:1588-1593.

12. Ito I, Ishida T, Hashimoto T, et al. Clinical comparison of Chlamydia pneumoniae pneumonia, ornithosis, and Mycoplasma pneumoniae pneumonia. [Article in Japanese] Nihon Kokyuki Gakkai Zasshi 2001;39:172-7.

13. Ito I, Ishida T, Osawa M, et al. Culturally verified Mycoplasma pneumoniae pneumonia in Japan: a long-term observation from 1979-99. Epidemiol Infect 2001;127:365-7.

14. HRCT Findings of Lung Disease. In: Webb WR, Muller NL and Naidich DP ed. *High-Resolution CT of the Lung* 2nd Ed. Lippincott Raven, 1996:41-108.

15. Loosli, Clayton G. Inter-alveolar communications in normal and pathologic mammalian lungs. AMA Arch Pathol 1937; 24:743-776.

16. Pulmonary bacterial infection. In: Spencer H and Hasleton PS eds. *Spencer's pathology of the lung*. 5th ed. McGraw-Hil, New York 1996: 189-256.

17. Rollins S, Colby T, Clayton F. Open lung biopsy in *Mycoplasma pneumoniae* pneumonia. Arch Pathol Lab Med 1986; 110:34-41.

18. Müller NL, Miller RR. Diseases of the bronchioles: CT and histopathologic findings. Radiology 1995; 196:3-12.

19. Murata K, Khan A, Herman PG. Pulmonary parenchymal disease: evaluation with high-resolution CT. Radiology 1989; 170:629-635.

20. Moazed TC, Kuo C, Patton DL, Grayston JT, Campbell LA. Experimental rabbit models of *Chlamydia pneumoniae* infection. Am J Pathol 1996;148:667-676.

21. Bryan CS. Pneumonia in Japan: another piece to a worldwide puzzle. Chest 1998;114:1509-11.

FIGURE LEGENDS

Figure 1. Mycoplasmal pneumonia in a 30-year-old woman. A transverse thin-section CT scan (1-mm collimation) through the level of the ventriculi of the heart shows ground-glass attenuation combined with centrilobular nodules (arrows) and thickened bronchial walls (arrowheads) in the left lower lobe.

Figure 2. Mycoplasmal pneumonia in a 27-year-old woman. A transverse thin-section CT scan (2-mm collimation) through the level of the dome of the right diaphragm demonstrates dominant centrilobular nodules in this patient. A small area of air-space consolidation with air-bronchogram is visible (arrow).

Figure 3. Mycoplasmal pneumonia in a 28-year-old man. A transverse thin-section CT scan (2-mm collimation) through the level of the ventriculi of the heart shows centrilobular nodules with poorly defined margins (arrows) located in the outer lung zone, focal areas of air-space consolidation, and ground-glass opacities. Air-space nodules more than 3 mm in size are also seen in this field.

Figure 4. Pneumococcal pneumonia in a 76-year-old man. A transverse thin-section CT scan (3-mm collimation) of the left lung at the level of the carina demonstrates ground-glass attenuation around air-space consolidation. Thickening of bronchovascular

bundles were also observed in bacterial pneumonias (arrows).

Figure 5. Pneumococcal pneumonia in a 60-year-old man. A transverse thin-section CT scan (1-mm collimation) of the right lung at the level of the carina shows an ill-defined cluster of airspace nodules with obscured vessels located in the outer third of the right upper lobe (arrows).

Figure 6. Pneumococcal pneumonia in a 29-year-old woman. A transverse thin-section CT scan (1-mm collimation) of the right lung at the level of the ventriculi of the heart shows air-space consolidations and interlobular septal thickenings (arrows) within ground-glass attenuation. Thickening of bronchial walls is also noted (arrowheads).

Figure 7. Receiver operating characteristic (ROC) curves from six-variable logistic regression models of the dependent variables "bacterial pneumonia" (model 1 and 2) and "mycoplasmal pneumonia" (model 3). Model 1 includes 125 cases with or without underlying lung disease (ULD) and model 2 includes 90 cases without ULD. Model 3 includes 56 cases diagnosed as either pneumococcal or mycoplasmal pneumonia without ULD. Sensitivity indicates the proportion of correctly classified patients as bacterial pneumonia in models 1 and 2 (pneumococcal pneumonia in model 3), and specificity indicates the proportion of correctly classified patients as non-bacterial pneumonia in

models 1 and 2 (mycoplasmal pneumonia in model 3). The areas under the ROC curves for models 1, 2, and 3 were 0.837, 0.885 and 0.953.

Table 1 - Etiology of 183 CAP episodes in which thin-section CT was obtained

Etiology	number of cases
Proven	128
Streptococcus pneumoniae	65 (51%)
without co-infections	59
with co-infections	6
Mycoplasma pneumoniae	20 (16%)
Haemophilus influenzae	12 (9%)
Chlamydia pneumoniae	7 (5%)
Streptococcus milleri group	4 (3%)
miscellaneous	18 (14%)
co-infections	2 (2%)
Unproven	55

Table 2 – Summary of thin-section CT findings

Finding	Interpretation criteria
areas of air-space consolidation	increased lung opacity with obscuration of vascular markings
areas of ground-glass attenuation	hazy increased lung opacity without obscuration of vascular markings
lobular opacity	opacity demarcated by interlobular borders
airspace nodules	small nodule 3-10 mm in diameter, ill-defined, accompanied with obscured small vessels
centrilobular nodules	micronodule less than 3 mm in diameter located in the centrilobular area
thickening of BVB	bronchial wall thickened by more than 25% of the diameter of the airway lumina
air-bronchogram	air-filled bronchus visible in parenchymal opacity
atelectasis	small or large section of collapsed lung without a gas-containing parenchyma
interlobular septal thickening	thickened septa 1-2 cm in length outlining part of or entire lobule
mediastinal adenopathy	mediastinal lymph nodes larger than 10 mm

BVB: bronchovascular bundles

Table 3 - Frequency of thin-section CT findings (1 of 2)

	Etiology*	Bacterial (n=94)			Non-bacterial (n=31)				
		Total	S.pn	H.inf	Total	M.pn	Chl.spp.	Un	Bac vs Non
Finding	N (%)	94	59	12	31	20	9	55	p**
Airspace nodules		41 (44)	25 (42)	6 (50)	19 (61)	16 (80)	3 (33)	25 (45)	0.101
outer zone dominant		24 (26)	15 (25)	4 (33)	2 (6)	1 (5)	1 (11)	11 (20)	0.023
Lobular opacity		33 (35)	24 (41)	3 (25)	21 (68)	18 (90)	1 (11)	20 (36)	0.002
Area of air-space consolidation (AS)		88 (94)	58 (98)	11 (92)	24 (77)	15 (75)	9 (100)	46 (84)	0.017
Area of ground-glass attenuation (GG)		80 (85)	50 (85)	8 (67)	26 (84)	15 (75)	9 (100)	49 (89)	1
Lobar pneumonia		28 (30)	20 (34)	0 (0)	10 (32)	7 (35)	3 (33)	18 (33)	0.82
Bilateral areas of AS or GG		40 (43)	25 (42)	5 (42)	7 (23)	3 (15)	3 (33)	25 (45)	0.056
GG located around AS		48 (51)	31 (53)	4 (33)	9 (29)	8 (40)	1 (11)	17 (31)	0.039

Table 3 (2 of 2)

Finding	Total (Bac)	S.pn	H.inf	Total (Non)	M.pn	Chl.spp.	Un	Bac vs Non
Air-bronchogram	85 (90)	58 (98)	9 (75)	28 (90)	20 (100)	8 (89)	46 (84)	1
Centrilobular nodules	26 (28)	16 (27)	4 (33)	19 (61)	15 (75)	2 (22)	18 (33)	0.001
as the prominent finding	2 (2)	0 (0)	1 (8)	7 (23)	5 (25)	1 (11)	2 (4)	0.001
outer zone dominant	10 (11)	6 (10)	1 (8)	12 (39)	10 (50)	1 (11)	10 (18)	0.001
bilateral	9 (10)	5 (8)	2 (17)	10 (32)	8 (40)	0 (0)	6 (11)	0.007
Thickening of BVB	49 (52)	33 (56)	6 (50)	25 (81)	18 (90)	5 (56)	29 (53)	0.001
Interlobular septal thickening	63 (67)	43 (73)	6 (50)	15 (48)	10 (50)	4 (44)	29 (53)	0.087
Mediastinal adenopathy	51 (54)	28 (47)	7 (58)	13 (42)	7 (35)	4 (44)	26 (47)	0.301
Atelectasis	8 (9)	6 (10)	1 (8)	7 (23)	7 (35)	0 (0)	6 (11)	0.054

*Analysis of 125 cases: from 128 cases with proven etiology, 3 cases were excluded. Ninety-four cases with bacterial pneumonia and 31 cases with non-bacterial pneumonia were included in the 125 cases.

**Fisher's exact probability test.

Abbreviations: S.pn, *Streptococcus pneumoniae*; M.pn, *Mycoplasma pneumoniae*' H.inf, *Haemophilus influenzae*; Chl. spp., *Chlamydia pneumoniae* (7 cases) and *Chlamydia psittaci* (2 cases); Un, unknown; Bac, bacterial pneumonia; Non, non-bacterial pneumonia; BVB, bronchovascular bundles.

Table 4 - Multiple logistic regression models of the three dependent variables

Model	1. Bacterial pneumonia with or without ULD*			2. Bacterial pneumonia without ULD**			3. Pneumococcal pneumonia without ULD***		
Independent variables	Beta	SE	p	Beta	SE	p	Beta	SE	p
Intercept	0.70	0.47	----	0.76	0.60	----	-1.37	1.99	----
ASN (outer zone predominance)	2.01	0.85	0.0054	1.99	0.96	0.021	3.68	2.02	0.015
Lobular opacity	-1.99	0.57	0.0002	-2.59	0.69	<0.0001	-3.62	1.35	0.0005
CLN (outer zone predominance)	-1.57	0.65	0.019	-2.18	0.85	0.0057	-3.84	1.46	0.0008
Bilateral areas of AS or GG	1.16	0.62	0.049	1.51	0.82	0.045	2.84	1.58	0.032
Thickening of ILS	1.04	0.57	0.061	1.08	0.68	0.098	1.67	1.12	0.11
GG located around AS	1.16	0.56	0.031	1.27	0.67	0.0497	----	----	----
Areas of GG	----	----	----	----	----	----	3.73	1.67	0.0052

*Analysis of 125 cases: from 128 cases with proven etiology, 3 cases were excluded. Ninety-four cases with bacterial pneumonia and 31 cases with non-bacterial pneumonia. ULD: underlying lung disease

**Analysis of 90 cases with proven etiology and without underlying lung diseases. Sixty-two cases with bacterial pneumonia and 28 cases with non-bacterial pneumonia.

***Analysis of 56 cases: cases infected with one of two representative pathogens and without underlying diseases. Thirty-six cases with pneumococcal pneumonia and 20 cases with mycoplasmal pneumonia.

Abbreviations: ASN, airspace nodules; CLN, centrilobular nodules; AS, air-space consolidation; GG, ground-glass opacity; ILS, interlobular septa.

Figure 1

Click here to download high resolution image

Figure 2

Click here to download high resolution image

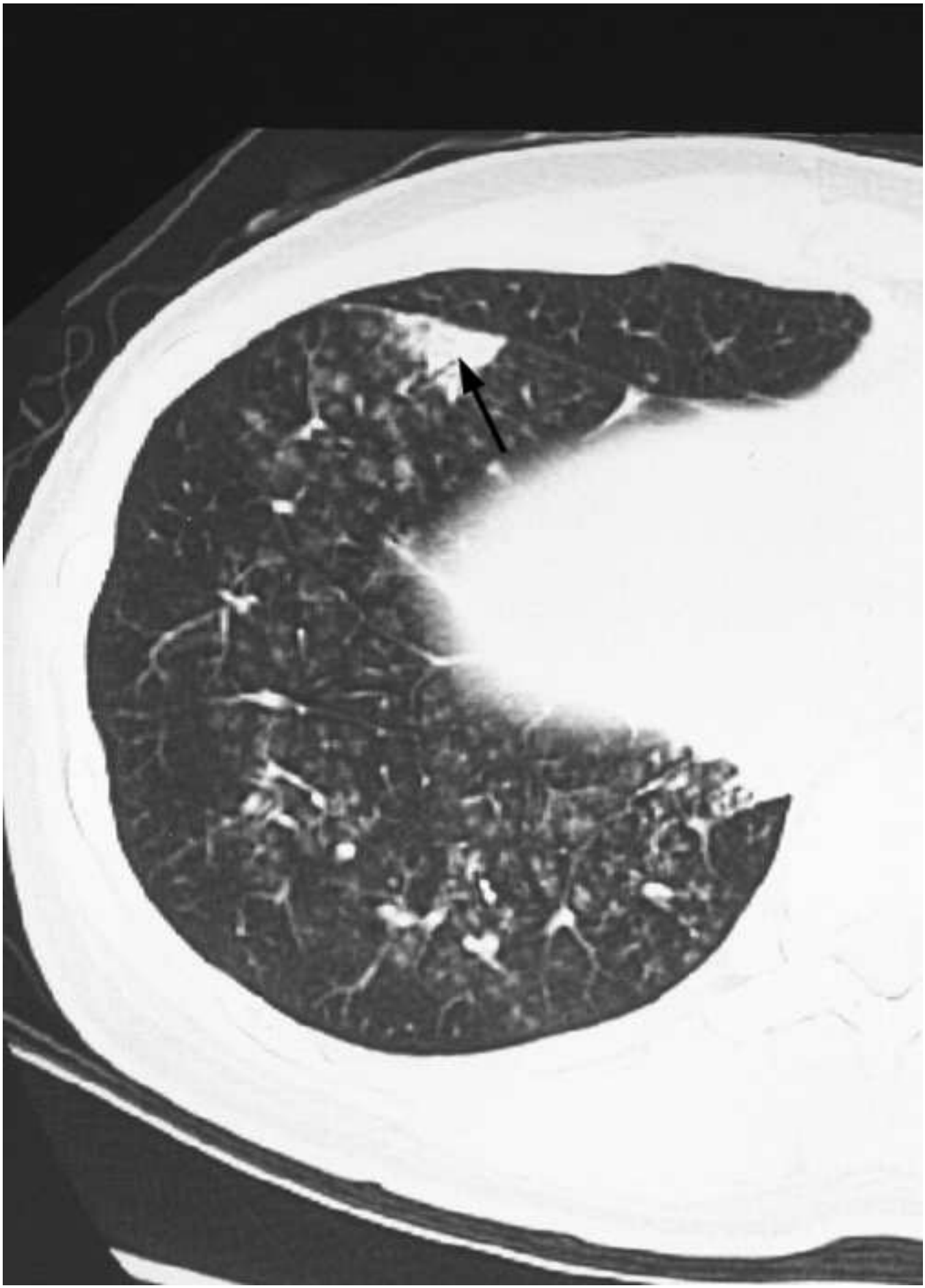

Figure 3

Click here to download high resolution image

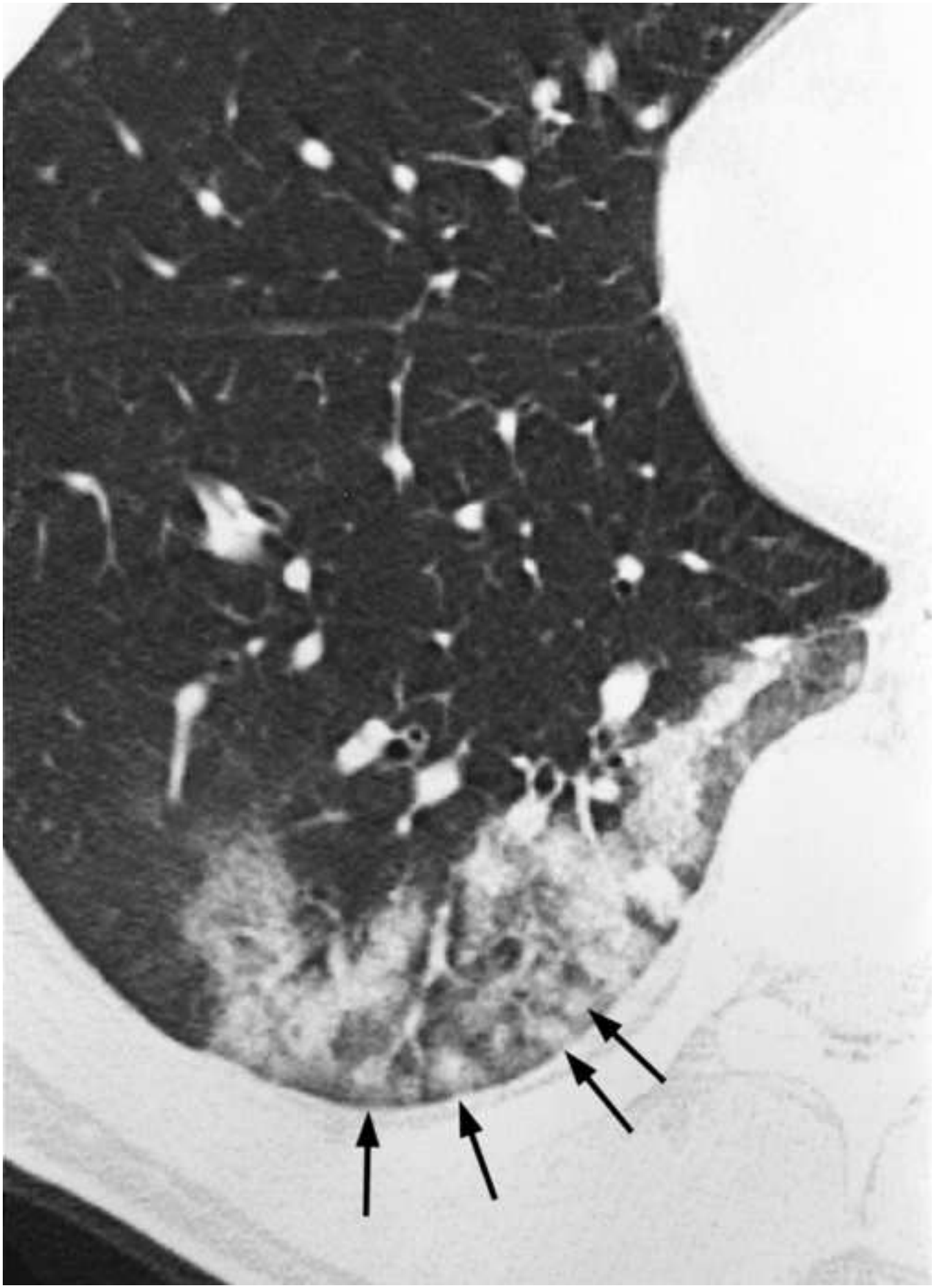

Figure 4

Click here to download high resolution image

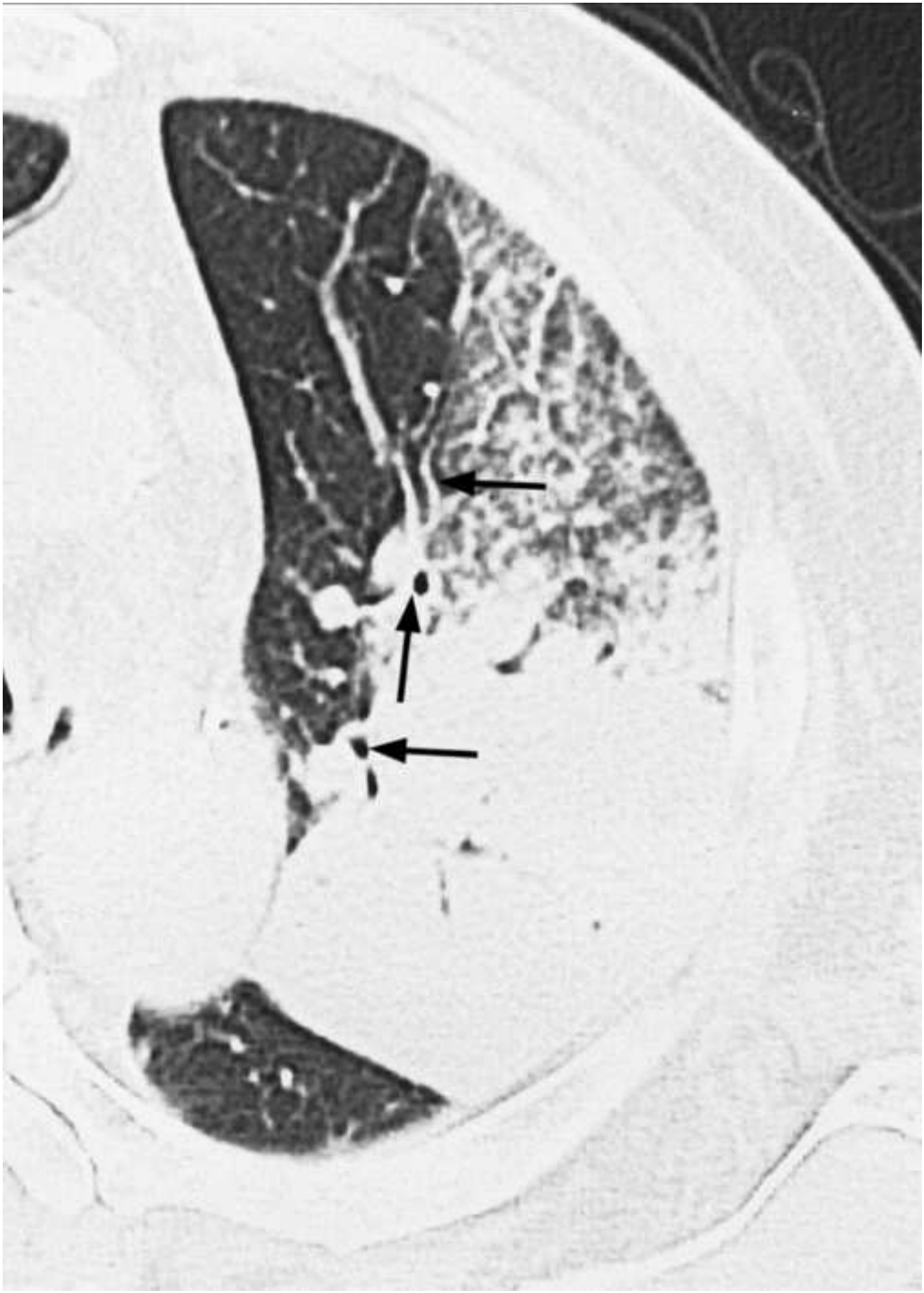

Figure 5

Click here to download high resolution image

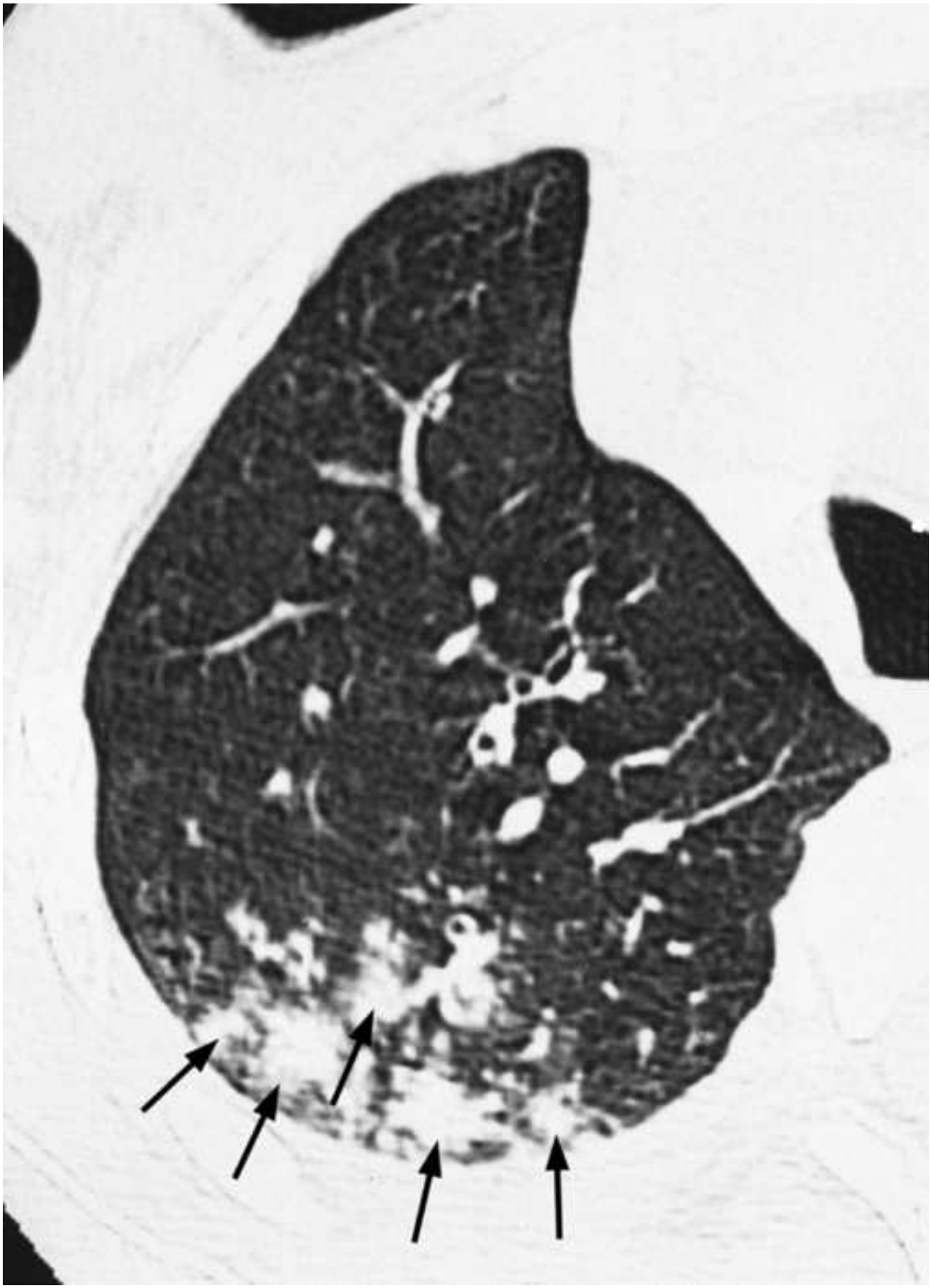

Figure 6

Click here to download high resolution image

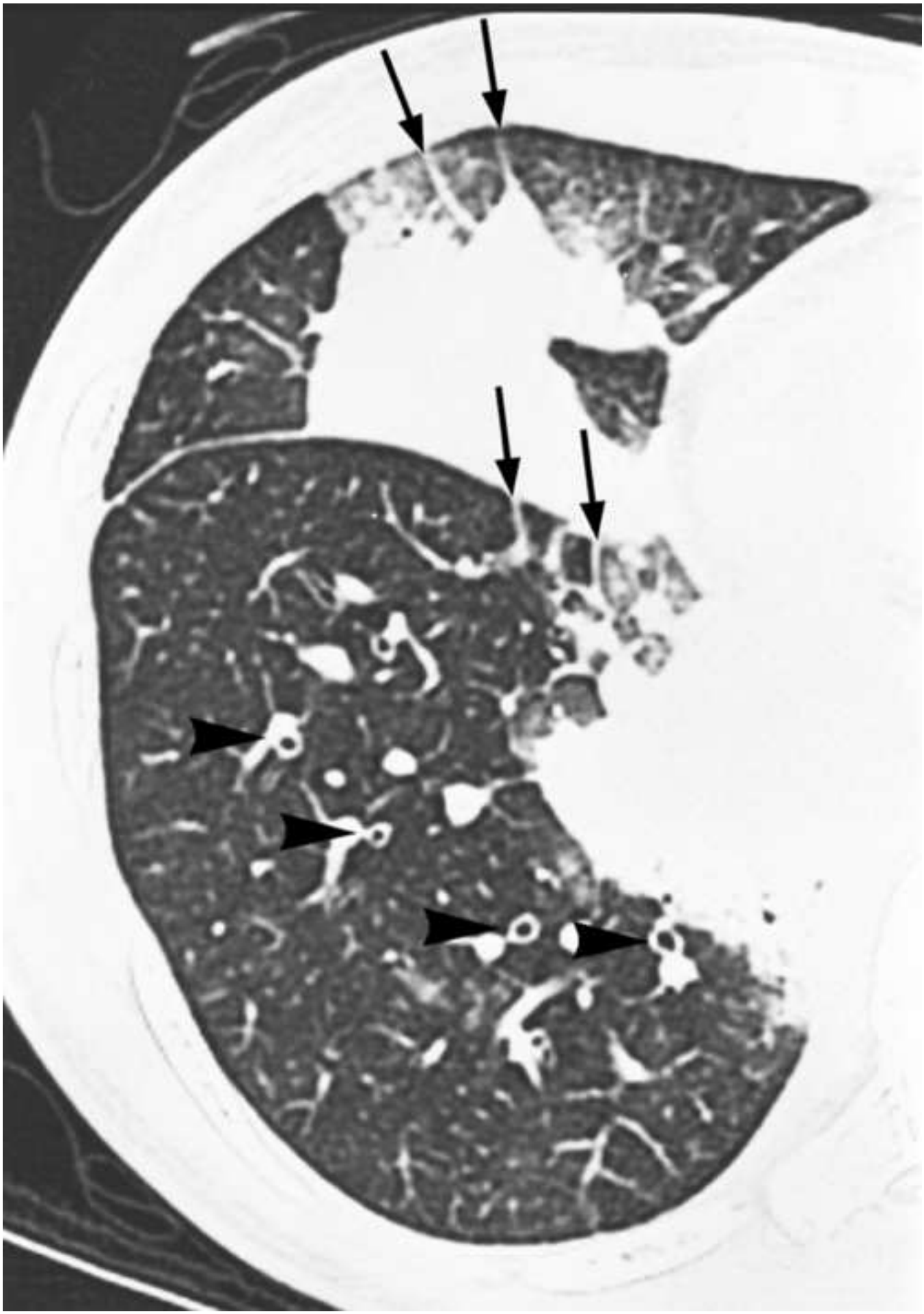

Figure 7

Click here to download high resolution image